

The fate of Reissner–Nordström–de Sitter black holes: nonequilibrium discharge and evaporation

Damien A. Easson

*Department of Physics, Arizona State University, Tempe, Arizona 85287, USA and
Beyond Center for Fundamental Concepts in Science,
Arizona State University, Tempe, Arizona 85287, USA*

Abstract

We develop an analytic semiclassical description of Reissner–Nordström–de Sitter (RN–dS) evaporation by combining a spherically reduced two-dimensional dilaton gravity model with Polyakov anomaly backreaction. The framework captures the causal and thermodynamic structure of the static patch and yields closed adiabatic evolution equations for the mass and charge. With an outward-oriented signed flux convention, the anomaly-induced Killing-energy flux is $\mathcal{F} = (N_{\text{eff}}/48\pi)(\kappa_b^2 - \kappa_c^2)$, while the full mass evolution is $\dot{M} = -\mathcal{F} + \Phi_b \dot{Q}$, with $\Phi_b = Q/r_b$. We prove analytically that along the entire sub-Nariai neutral Schwarzschild–de Sitter branch $\kappa_b > \kappa_c$, so that neutral black holes lose mass monotonically. Schwinger pair production provides the discharge channel. In the rapid-discharge regime, controlled charged trajectories become effectively neutral on a timescale short compared with the anomaly-driven Hawking mass-loss time and then follow the neutral SdS channel toward empty de Sitter space. The classical lukewarm locus $T_b = T_c$ is therefore only the nullcline of the anomaly-induced heat flux. Once discharge is included, the electromagnetic work term tilts the full semiclassical vector field away from this curve, so the lukewarm locus is not an invariant trajectory of the coupled flow. When sufficiently light charged species provide an operative rapid-discharge channel, the distinguished classical loci—cold/extremal, charged Nariai, ultracold, and lukewarm—are not semiclassical attractors for controlled nondegenerate trajectories. These results give an adiabatically backreacted derivation of the RN–dS evaporation endpoint in the regime controlled by anomaly-induced flux and rapid charge discharge, and provide the semiclassical background for generalized-second-law monotonicity and conservative quantum-extremal-surface/island estimates.

I. INTRODUCTION

Black-hole thermodynamics in de Sitter (dS) space is intrinsically nonequilibrium. A black hole in a static patch coexists with a cosmological horizon, and the two horizons generally have different surface gravities, κ_b and κ_c , and hence different temperatures $T_h = \kappa_h/2\pi$. Understanding how such a two-horizon system evolves under Hawking radiation, charge loss, and horizon motion is therefore essential for a consistent semiclassical account of black holes in an accelerating universe.

The neutral Schwarzschild–de Sitter (SdS) problem has recently been clarified from several complementary perspectives. Four-dimensional greybody-resolved calculations and near-Nariai backreaction analyses have addressed important aspects of black-hole evaporation in de Sitter space [1, 2]. In a Lorentzian two-dimensional anomaly-induced description, neutral SdS evaporation admits an analytic nonequilibrium flux law and evolves monotonically toward empty de Sitter space [3]. A complementary Euclidean perspective [4], has shown that once an observer is included, the Euclidean Nariai geometry carries the phase appropriate to black-hole nucleation. The authors also argued that the Bousso–Hawking anti-evaporation branch [5] is a singular-state artifact: for horizon-smooth states, near-Nariai black holes evaporate thermally and relax back to empty de Sitter. These results clarify the neutral problem, but they do not determine the Lorentzian evolution of charged Reissner–Nordström–de Sitter (RN–dS) black holes, where charge loss, electromagnetic work, and the full mass/charge phase space become essential.

In this paper we construct an analytic semiclassical model for the joint discharge and evaporation of charged black holes in de Sitter space. The starting point is the spherical reduction of four-dimensional Einstein–Maxwell– Λ gravity, supplemented by the Polyakov anomaly action [6] for the universal two-dimensional conformal contribution to the radial energy flux. With positive flux defined outward from the black-hole horizon toward the cosmological horizon, this sector fixes the horizon-to-horizon Killing-energy flux to be proportional to $\kappa_b^2 - \kappa_c^2$. The charged problem then requires one additional ingredient: when Q evolves, the mass equation contains the electromagnetic work term, $\dot{M} = -\mathcal{F} + \Phi_b \dot{Q}$. Together with a near-horizon Schwinger discharge law, this gives a closed adiabatic system for (M, Q) .

Classical RN–dS geometry contains several celebrated loci: the cold/extremal branch, the

charged Nariai branch, the ultracold point, and the lukewarm curve $T_b = T_c$ [7–10]. These geometries are often discussed as candidate equilibrium or endpoint configurations, but such interpretations are based on static solution space rather than on the time-dependent semiclassical flow. Earlier analyses of charged black-hole evaporation and pair production [11–15] treated local fluxes or fixed backgrounds, while thermodynamic, Euclidean, instanton, and “shark-fin” analyses mapped the RN–dS parameter space and its distinguished loci using static or quasistatic methods [8, 10, 16–19]. Observer-normalized first laws are essential for the local thermodynamic interpretation of these loci, especially near Nariai; here, by contrast, κ_b and κ_c denote the Killing surface gravities entering the conserved anomaly-induced Killing-energy current. Ref. [20] derived general evolution constraints from effective energy and charge fluxes in the context of the *Festina Lente* proposal, and near-extremal de Sitter black holes were studied in [21] using a Schwarzsian effective theory. These works provide important complementary analyses, but none produced the closed anomaly-induced horizon-to-horizon flow studied here.

The key distinction is dynamical. Heat capacities, fixed-temperature ensembles, and quasistatic first-law relations do not determine the flow generated by the coupled equations for M and Q . In particular, the classical lukewarm curve remains important, but only as the nullcline of the Polyakov heat flux: it is the locus where $\kappa_b = \kappa_c$ and hence the anomaly flux vanishes. It is not a full-flow mass nullcline once $\dot{Q} \neq 0$, because the mass equation still contains the electromagnetic work term $\Phi_b \dot{Q}$. Thus the dynamical status of the lukewarm curve must be assessed in the full (M, Q) system as we discuss below.

The local input for the discharge channel is supported by the classic Schwinger-discharge picture of charged black holes [11] and by recent worldline-instanton work. Ref. [22] computed the radial pair-production profile for extremal Reissner–Nordström black holes in asymptotically flat space and found that Schwinger production is exponentially localized within a Compton wavelength of the horizon. Their analysis shows that the dominant contribution to the discharge rate is controlled by the near-horizon electric field, with contributions from larger radii exponentially suppressed. We use this as motivation for the horizon-local discharge law in the RN–dS static patch, while embedding it in a global two-horizon energy-balance equation.

The central result is a two-stage endpoint mechanism. First, in the rapid-discharge regime, Schwinger pair production drives $|Q| \rightarrow 0$ on a timescale parametrically shorter

than the anomaly-induced Hawking mass-loss time. Second, once the trajectory reaches the neutral neighborhood, the neutral SdS ordering takes over. We prove in Appendix A that

$$\kappa_b(M, 0) > \kappa_c(M, 0), \quad 0 < M < M_N,$$

so the anomaly-induced flux drives monotonic mass loss along the neutral branch. Thus controlled rapid-discharge trajectories evolve toward the empty de Sitter endpoint rather than toward a cold, charged Nariai, ultracold, or lukewarm remnant. No global ordering of κ_b and κ_c in the charged RN–dS family is assumed or required; indeed, the charged family contains the lukewarm locus where the anomaly flux vanishes.

Our analysis clarifies the relation to recent near-extremal and lukewarm studies. Several works have emphasized the need for a backreacted one-loop treatment incorporating Hawking flux, electromagnetic discharge, and observer-based energy conservation [23]. The present construction supplies this missing ingredient within a controlled spherically symmetric adiabatic model: the Polyakov sector fixes the conserved horizon-to-horizon flux, the Schwinger law supplies the charge-loss channel, and the resulting phase-space flow determines which classical loci can actually be approached dynamically. The same time-dependent background provides the input for a conservative island/QES estimate. The island prescription and its role in black-hole evaporation are now well established [24–26], and related questions in cosmological and de Sitter settings have been explored in Refs. [27–30]. We do not attempt a microscopic derivation of the exact fine-grained Page curve; rather, we use the evaporation dynamics to identify the background on which the late-time no-island/island saddle competition should be evaluated.

The remainder of the paper is organized as follows. Section II sets up the spherical reduction of Einstein–Maxwell– Λ gravity and fixes the RN–dS conventions used throughout. Section III derives the anomaly-induced horizon-to-horizon flux and introduces the full mass evolution equation, including the electromagnetic work term. Section IV establishes the corresponding coarse-grained two-horizon entropy balance. Section V constructs the coupled (M, Q) evolution system and the corresponding phase portrait. Section VI analyzes the cold/extremal, charged Nariai, ultracold, and lukewarm loci in the full flow. Section VII states the endpoint theorem for the controlled rapid-discharge regime. Section VIII gives the information-theoretic interpretation in terms of a conservative island/QES estimate.

Appendix A proves the neutral SdS surface-gravity ordering, and Appendix B derives the conserved-current origin of the Polyakov ($\kappa_b^2 - \kappa_c^2$) flux structure.

II. DIMENSIONAL REDUCTION AND EFFECTIVE 2D THEORY

We begin with Einstein–Maxwell– Λ gravity in four dimensions,

$$S_4 = \frac{1}{16\pi G_4} \int d^4x \sqrt{-g} (R - 2\Lambda) - \frac{1}{16\pi} \int d^4x \sqrt{-g} F_{\mu\nu} F^{\mu\nu}, \quad (1)$$

in Gaussian units where the RN potential takes its standard form. Imposing spherical symmetry, $ds^2 = g_{ab}(x)dx^a dx^b + r(x)^2 d\Omega_2^2$, and defining the dilaton $X = r^2$, one finds after integrating over S^2 (up to a total derivative) the standard spherically reduced gravity form [31–33]:

$$S_2 = \frac{1}{4G_4} \int d^2x \sqrt{-g} \left[XR + U(X)(\nabla X)^2 + 2V(X) \right], \quad (2)$$

with

$$U(X) = \frac{1}{2X}, \quad V(X) = 1 - \Lambda X - \frac{G_4 Q^2}{X}. \quad (3)$$

Here Q denotes the conserved electric charge after eliminating the two-dimensional Maxwell field at fixed charge. With our normalization this gives the effective charge contribution $-G_4 Q^2/X$, and the two-dimensional action is written with a $+2V(X)$ term. A Weyl rescaling to the frame

$$\tilde{g}_{ab} = X^{1/2} g_{ab}$$

removes the dilaton kinetic term and gives

$$\tilde{V}(X) = X^{-1/2} \left(1 - \Lambda X - \frac{G_4 Q^2}{X} \right). \quad (4)$$

In the areal-radius coordinate $r = \sqrt{X}$, we define the radial primitive entering the Schwarzschild-gauge solution by

$$W'(r) = V(r^2). \quad (5)$$

For the potential above,

$$W(r) = r - \frac{\Lambda r^3}{3} + \frac{G_4 Q^2}{r}. \quad (6)$$

This radial primitive $W(r)$ is the quantity entering the four-dimensional Schwarzschild-gauge blackening function. With this convention the equation $(r\xi)' = V(r^2) = W'(r)$ directly reproduces the four-dimensional RN–dS metric.

The static solution then has

$$ds^2 = -\xi(r) dt^2 + \xi(r)^{-1} dr^2 + r^2 d\Omega_2^2, \quad (7)$$

$$\xi(r; M, Q) = \frac{W(r) - 2G_4 M}{r} = 1 - \frac{2G_4 M}{r} + \frac{G_4 Q^2}{r^2} - \frac{\Lambda r^2}{3}, \quad (8)$$

which fixes the normalization used in this paper.

Conventions.— We adopt units $c = \hbar = 1$ throughout, while keeping G_4 explicit. For generic charged nondegenerate RN–dS data, the static patch has three positive roots

$$0 < r_- < r_b < r_c,$$

corresponding respectively to the inner/Cauchy, black-hole/event, and cosmological horizons. The surface gravities are

$$\kappa_h = \frac{1}{2} |\xi'(r_h)|, \quad h = b, c. \quad (9)$$

The cold/extremal branch is defined by $r_- = r_b$, the charged Nariai branch by $r_b = r_c$, and the ultracold point by $r_- = r_b = r_c$. The neutral Nariai mass and maximum RN–dS charge scale are

$$M_{\mathcal{N}} = \frac{1}{3G_4\sqrt{\Lambda}}, \quad Q_{\mathcal{E}} = \frac{1}{2\sqrt{G_4\Lambda}}, \quad (10)$$

and the phase-space variables are

$$\mu = \frac{M}{M_{\mathcal{N}}}, \quad q = \frac{Q}{Q_{\mathcal{E}}}. \quad (11)$$

We take $Q \geq 0$ in the displayed phase portrait; the $Q < 0$ half-plane is obtained by charge conjugation. In formulas valid with either sign of Q , the Schwinger rate is written with $|Q|$ and $\text{sgn}(Q)$.

For the neutral Schwarzschild–de Sitter case ($Q = 0$), it is convenient to express the surface gravities in terms of the three real roots ($r_0 < 0 < r_b < r_c$) of $\xi(r)$. Using the

factorization

$$\xi(r) = -\frac{\Lambda}{3r} (r - r_b)(r - r_c)(r - r_0),$$

and the definition $\kappa_h = \frac{1}{2}|\xi'(r_h)|$, one obtains the closed forms

$$\kappa_b = \frac{(r_c - r_b)(2r_b + r_c)}{2r_b(r_b^2 + r_b r_c + r_c^2)}, \quad (12)$$

$$\kappa_c = \frac{(r_c - r_b)(r_b + 2r_c)}{2r_c(r_b^2 + r_b r_c + r_c^2)}. \quad (13)$$

We use these expressions repeatedly in analyzing the semiclassical flow.

A. 2D effective field theory perspective

The reduction from 4D Einstein–Maxwell– Λ gravity to the 2D dilaton theory in Eq. (2) may be viewed as a controlled effective field theory for the spherically symmetric, semiclassical dynamics of the RN–dS geometry. The dilaton encodes the areal radius of the transverse S^2 , while higher spherical harmonics are integrated out. The blackening function (8) and dilaton potential $\tilde{V}(X)$ in Eq. (4) reproduce the exact classical spherically symmetric sector of the four-dimensional theory.

The Polyakov anomaly term (14) then supplies the universal pure-conformal contribution to the two-dimensional trace anomaly for N conformal fields. In this pure Polyakov sector, the associated Killing-energy current is conserved on each static patch and depends only on the two-dimensional metric. Charge therefore enters the anomaly-induced flux only through the geometry $\xi(r; M, Q)$, and hence through the horizon data $\kappa_b(M, Q)$ and $\kappa_c(M, Q)$, rather than through a separate charge-specific anomaly coupling.

This is the controlled approximation used below. In a more complete spherically reduced treatment, dilaton-dependent anomaly terms, greybody factors, and higher-derivative corrections can modify state-dependent details and effective coefficients [34–36]. The endpoint argument requires only that, after rapid discharge has driven the solution into an effectively neutral neighborhood, the neutral net flux retain the sign fixed by the SdS ordering proved in Appendix A.

To include backreaction from N conformal fields, we add the Polyakov anomaly term

[6, 37–39],

$$S_{\text{anom}} = -\frac{N}{96\pi} \int d^2x \sqrt{-g} R \square^{-1} R, \quad (14)$$

giving $\langle T^\mu{}_\mu \rangle = (N/24\pi)R$. In the adiabatic approximation, the geometry is treated at each advanced time as an instantaneous static RN–dS patch,

$$ds^2 = -\xi(r; M(v), Q(v)) dv^2 + 2 dv dr. \quad (15)$$

The corresponding instantaneous Killing vector is $\zeta^\mu = (\partial_v)^\mu$, equivalently $(\partial_t)^\mu$ in Schwarzschild coordinates. For the covariantly conserved Polyakov stress tensor, the associated Killing-energy current

$$J^\mu = -T^\mu{}_\nu \zeta^\nu$$

is conserved on each fixed static patch,

$$\nabla_\mu J^\mu = 0,$$

up to higher adiabatic corrections in the slowly evolving geometry.

In what follows we make systematic use of the anomaly-induced Killing-energy flux derived for the neutral Schwarzschild–de Sitter reduction in Ref. [3]. Because the Polyakov term depends only on the two-dimensional metric, turning on charge introduces no new anomaly couplings: the charged RN–dS case differs only through its geometry, encoded in $\xi(r; M, Q)$ and the associated horizon surface gravities, and requires no new structural ingredient beyond replacing the neutral metric function by Eq. (8).

III. SEMICLASSICAL FLUXES AND COUPLED EVOLUTION

We work in the Unruh–de Sitter state, regular on the future black-hole and cosmological horizons in the appropriate chiral sectors. We denote by

$$\mathcal{F}(M, Q) = \frac{N_{\text{eff}}}{48\pi} \left(\kappa_b^2(M, Q) - \kappa_c^2(M, Q) \right) \quad (16)$$

the outward-oriented signed Polyakov flux; positive values correspond to energy flow from the black-hole horizon toward the cosmological horizon. The full adiabatic mass evolution

during discharge is

$$\dot{M} = -\mathcal{F} + \Phi_b \dot{Q}, \quad \Phi_b = \frac{Q}{r_b}, \quad (17)$$

where Φ_b is the black-hole horizon potential in our adopted gauge.

The sign of the work term follows from the black-hole horizon first law. Differentiating $\xi(r_b; M, Q) = 0$ at fixed Λ gives

$$0 = \xi'(r_b) \dot{r}_b - \frac{2G_4}{r_b} \dot{M} + \frac{2G_4 Q}{r_b^2} \dot{Q}.$$

Using $\xi'(r_b) = 2\kappa_b$, $S_b = \pi r_b^2/G_4$, and $T_b = \kappa_b/(2\pi)$, this becomes

$$\dot{M} = T_b \dot{S}_b + \Phi_b \dot{Q}, \quad \Phi_b = \frac{Q}{r_b}.$$

The outward Polyakov flux removes heat from the black-hole horizon, $T_b \dot{S}_b = -\mathcal{F}$, giving Eq. (17).

For fixed charge this reduces to the anomaly-only contribution

$$\dot{M}_H = -\mathcal{F}. \quad (18)$$

For arbitrary sign of Q , a useful horizon-local parametrization of the Schwinger discharge channel is

$$\dot{Q} = -\bar{\beta}_{\text{Sch}} \ell_* \frac{e_{\text{eff}}^2 |Q|}{2\pi r_b^2} \text{sgn}(Q) \exp\left[-\frac{\pi m_{\text{eff}}^2 r_b^2}{e_{\text{eff}} |Q|}\right], \quad (19)$$

for the lightest available charged species of mass m_{eff} and charge e_{eff} . Here ℓ_* is an effective matching length associated with the near-horizon production region, while the dimensionless positive coefficient $\bar{\beta}_{\text{Sch}}$ absorbs greybody factors, species degeneracies, dimensional-reduction effects, and the matching between the local four-dimensional pair-production rate and the net charge current.¹

Equation (19) should be understood as an effective two-dimensional horizon-local current ansatz, not as a first-principles integration of the four-dimensional volume production rate. The endpoint argument uses only its robust sign,

$$\dot{Q} \text{sgn}(Q) < 0,$$

¹ The factor ℓ_* restores the effective length scale that is lost when the four-dimensional near-horizon production region is compressed into a horizon-local two-dimensional charge-current ansatz.

together with the assumed rapid-discharge hierarchy $t_Q \ll t_M$. For the phase portrait we display $Q \geq 0$, in which case the same formula simply gives $\dot{Q} < 0$. Equations (17) and (19) determine the coupled flow in (M, Q) space.

Remark on near-horizon locality.— The use of a near-horizon Schwinger law in Eq. (19) is supported by the worldline-instanton analysis of Lin and Shiu [22], who computed the full radial dependence of $\Gamma(r)$ for extremal Reissner–Nordström and found that pair production is exponentially localized within a Compton wavelength of the black-hole horizon. Their results show that the dominant contribution to the discharge rate is governed by the near-horizon region and that contributions from larger radii are negligibly small. Incorporating this localized discharge into the global two-horizon flux law (17) is a central component of the present work.

IV. NONEQUILIBRIUM THERMODYNAMICS

For the two-derivative Einstein–Maxwell– Λ theory considered here, the Wald entropy reduces to the area entropy,

$$S_h = \frac{A_h}{4G_4} = \frac{\pi r_h^2}{G_4},$$

and $T_h = \kappa_h/2\pi$. For nondegenerate horizons and fixed Λ , the adiabatic horizon first laws are

$$T_b \dot{S}_b = \dot{M} - \Phi_b \dot{Q}, \quad T_c \dot{S}_c = -\dot{M} + \Phi_c \dot{Q}, \quad \Phi_h = \frac{Q}{r_h}.$$

Using the full semiclassical mass evolution equation (17) one finds

$$T_b \dot{S}_b = -\mathcal{F}, \quad T_c \dot{S}_c = \mathcal{F} + (\Phi_c - \Phi_b) \dot{Q}.$$

Hence

$$\dot{S}_b + \dot{S}_c = \mathcal{F} \left(\frac{1}{T_c} - \frac{1}{T_b} \right) + \frac{(\Phi_c - \Phi_b) \dot{Q}}{T_c}.$$

Since

$$\mathcal{F} = \frac{N_{\text{eff}}}{48\pi} (\kappa_b^2 - \kappa_c^2)$$

with positive coefficient, and since $T_h = \kappa_h/2\pi > 0$ for nondegenerate horizons, \mathcal{F} has the same sign as $T_b - T_c$. Therefore

$$\mathcal{F} \left(\frac{1}{T_c} - \frac{1}{T_b} \right) = \mathcal{F} \frac{T_b - T_c}{T_b T_c} \geq 0.$$

The second term is also nonnegative during Schwinger discharge, since $(\Phi_c - \Phi_b)\dot{Q} \geq 0$ for either sign of Q . Thus the adiabatic two-horizon entropy balance is monotonic in the discharging regime. This gives the coarse-grained horizon generalized-second-law balance. The relation to fine-grained entropy and the corresponding island/QES saddle competition is discussed separately in Sec. VIII.

Killing flux versus observer-normalized thermodynamics. — The surface gravities κ_b and κ_c appearing in Eq. (16) are Killing surface gravities in the normalization used to define the conserved Polyakov Killing-energy current. They should not be confused with observer-normalized temperatures used in physical static-patch first laws. In de Sitter black-hole thermodynamics, changing the normalization of the timelike Killing vector corresponds to choosing a different static observer; in particular, the Bousso–Hawking normalization can assign finite temperatures to the Nariai throat even though the conventional static-patch Killing surface gravities vanish there [19]. The present flux law instead tracks the signed conserved Killing-energy transfer between the two outer horizons. A common positive rescaling of the Killing vector rescales both outer surface gravities and the corresponding Killing-energy variable consistently, but it does not alter the lukewarm nullcline $\kappa_b = \kappa_c$, the neutral ordering $\kappa_b > \kappa_c$, or the direction of the phase-space flow after all quantities are expressed in the same normalization. Thus observer-normalized first-law analyses and the present Killing-current evolution answer complementary questions: the former concern local thermodynamic response and heat capacities, while the latter determines the direction of semiclassical horizon-to-horizon energy transport.

V. SEMICLASSICAL EVOLUTION IN THE (M, Q) PLANE

For RN–dS, semiclassical evolution in the static patch is governed by two coupled processes: anomaly-induced Hawking radiation and Schwinger pair production of charged particles. These give rise to a dynamical system for the black-hole mass $M(v)$ and charge $Q(v)$

as functions of the advanced time v .

We adopt the geometric conventions summarized in Sec. II. For a nondegenerate charged RN–dS geometry in the interior of the physical static-patch domain, there are three positive roots

$$0 < r_-(M, Q) < r_b(M, Q) < r_c(M, Q),$$

corresponding to the inner, black-hole, and cosmological horizons. The outer horizons have surface gravities $\kappa_b(M, Q)$ and $\kappa_c(M, Q)$. The neutral Schwarzschild–de Sitter branch is obtained as the $Q \rightarrow 0$ boundary of this family, where only the black-hole and cosmological horizons remain. Along that neutral branch, Appendix A proves

$$\kappa_b(M, 0) > \kappa_c(M, 0) > 0, \quad 0 < M < M_{\mathcal{N}}.$$

This neutral ordering will be used below after the discharge dynamics has driven the system into an effectively neutral neighborhood.

A. Anomaly-induced Hawking flux

As in the neutral SdS case [3], integrating out N conformal matter fields and including the Polyakov action yields a conserved Killing flux in the Unruh–de Sitter state. The coefficient of the two-dimensional Polyakov anomaly is N , while the effective coefficient entering the four-dimensional matched flux law is denoted N_{eff} . With the outward-oriented signed convention of Eq. (16), the Polyakov contribution is \mathcal{F} . In the pure Polyakov sector, charge modifies this flux only through the geometry $\xi(r; M, Q)$ and hence through the horizon data $\kappa_b(M, Q)$ and $\kappa_c(M, Q)$. The anomaly-only mass change at fixed charge is

$$\dot{M}_{\text{H}} = -\mathcal{F}.$$

When discharge is present, the total mass evolution is instead the full energy-balance relation (17).

By the neutral SdS ordering proved in Appendix A, the anomaly flux is positive along

the entire sub-Nariai neutral branch, leading to

$$\dot{M}_{\text{H}}(M, 0) = -\mathcal{F}(M, 0) < 0, \quad 0 < M < M_{\mathcal{N}},$$

so neutral SdS black holes lose mass monotonically.

For $Q \neq 0$, however, the sign of $\kappa_b^2 - \kappa_c^2$ need not be fixed. It vanishes on the classical lukewarm locus, and on the side where $\kappa_b < \kappa_c$ the outward-oriented Polyakov flux is negative, so the anomaly-only contribution to the mass change satisfies

$$\dot{M}_{\text{H}} > 0.$$

This corresponds to a temporary inward Killing-energy current from the cosmological horizon toward the black-hole horizon in the effective two-horizon balance. In the full system, Eq. (17) shows that this positive anomaly-only mass contribution competes with the electromagnetic work term. During discharge, $\Phi_b \dot{Q} \leq 0$, while the charge equation still drives $|Q|$ downward. Thus an initially negative Polyakov flux does not obstruct the endpoint mechanism in the rapid-discharge regime: the trajectory is driven across the lukewarm nullcline into an effectively neutral neighborhood, where the neutral ordering, together with continuity near $Q = 0$, fixes the subsequent positive sign of the Polyakov flux and hence the remaining mass loss.

B. Schwinger discharge of the black-hole charge

The electric field near the black-hole horizon sources Schwinger pair production of charged particles [40]. For a species of mass m and charge e with $|eQ| \gg 1$, the local pair creation rate per unit four-volume is approximately

$$\Gamma_{\text{Sch}}(M, Q) \sim \frac{(eE_b)^2}{4\pi^3} \exp\left[-\frac{\pi m^2}{eE_b}\right], \quad (20)$$

where $E_b = |Q|/r_b^2$ in the conventions of Eq. (8). Motivated by the near-horizon localization of the Schwinger process, we parametrize the net horizon-local discharge current by the sign-safe effective law (19). The dimensionless coefficient $\bar{\beta}_{\text{Sch}}$ absorbs the radial profile of the production region, greybody factors, species degeneracies, dimensional-reduction effects, and

the matching between the local four-dimensional pair-production rate and the net charge current; the associated microscopic matching length is denoted ℓ_* . Crucially,

$$\dot{Q}_{\text{Sch}}(M, Q) \text{sgn}(Q) < 0, \quad (21)$$

so Schwinger discharge always decreases the magnitude of the charge,

$$\frac{d}{dv}|Q(v)| < 0, \quad (22)$$

until the black hole becomes effectively neutral.

In the physically relevant regime with at least one light charged species obeying $eE_b \gtrsim m^2$ over a substantial portion of the evolution, the exponential in (19) is not strongly suppressed, and the associated discharge timescale is parametrically shorter than the Hawking mass-loss timescale. We return to this hierarchy of timescales below.

C. Dimensionless dynamical system

It is convenient to introduce dimensionless variables adapted to the RN–dS “shark-fin” parameter space. We use the de Sitter radius $L = \sqrt{3/\Lambda}$ as the time scale and the phase-space scales in Eq. (10):

$$\mu = \frac{M}{M_{\mathcal{N}}}, \quad q = \frac{Q}{Q_{\mathcal{E}}}, \quad \tau = \frac{v}{L}. \quad (23)$$

The admissible nondegenerate static-patch geometries form a bounded domain \mathcal{D} in the (μ, q) plane.

In these variables the full semiclassical flow is

$$\frac{d\mu}{d\tau} = F(\mu, q) \equiv \frac{L}{M_{\mathcal{N}}} \left[-\mathcal{F}(M, Q) + \Phi_b(M, Q)\dot{Q}(M, Q) \right], \quad (24)$$

$$\frac{dq}{d\tau} = G(\mu, q) \equiv \frac{L}{Q_{\mathcal{E}}}\dot{Q}(M, Q), \quad (25)$$

with $M = M_{\mathcal{N}}\mu$, $Q = Q_{\mathcal{E}}q$, and \dot{Q} given by Eq. (19). Here the electromagnetic work term $\Phi_b\dot{Q}$ is present in the mass equation. The above also makes clear that the classical lukewarm locus $\kappa_b = \kappa_c$ is only the anomaly-flux nullcline $\mathcal{F} = 0$; it is not the full mass nullcline when

$\dot{Q} \neq 0$.

The sign information used below is

$$G(\mu, q) \operatorname{sgn}(q) < 0, \quad \Phi_b \dot{Q} \leq 0, \quad F(\mu, 0) < 0 \quad (0 < \mu < 1), \quad (26)$$

where the last inequality is the neutral SdS result. No global sign is assumed for the anomaly term away from the neutral line.

D. Phase portrait

The sign structure (26) determines the robust part of the qualitative phase portrait in the physical domain \mathcal{D} . For $q > 0$ one has $G < 0$, while for $q < 0$ one has $G > 0$; hence the charge component of the vector field always points toward the neutral line. Along $q = 0$ the charge is frozen and the mass decreases monotonically by the neutral SdS theorem. Away from the neutral line the anomaly term can change sign across the lukewarm locus, but the work term $\Phi_b \dot{Q}$ is always nonpositive during discharge, and in the rapid-discharge regime the charge motion dominates before the mass changes appreciably.

Thus trajectories in the regime $t_Q \ll t_M$ are first driven toward an effectively neutral neighborhood of $q = 0$ and then follow the neutral channel toward lower μ . In the presence of at least one light charged species with unsuppressed Schwinger production, the characteristic discharge timescale

$$t_Q \sim \frac{|Q|}{|\dot{Q}_{\text{Sch}}|} \quad (27)$$

is parametrically shorter than the Hawking mass-loss timescale

$$t_M \sim \frac{M}{|\dot{M}_{\text{H}}|}, \quad (28)$$

so the trajectory first experiences a rapid neutralization burst, $|q| \rightarrow 0$, followed by a slower evolution along the neutral SdS channel $\mu \rightarrow 0$.

The essential point is that rapid discharge turns the late-time problem into the neutral SdS problem: once Q is macroscopically negligible, the neutral ordering proved in Appendix A fixes the sign of the remaining anomaly-driven Hawking evolution.

We next use this phase-portrait to identify the possible endpoints of the semiclassical

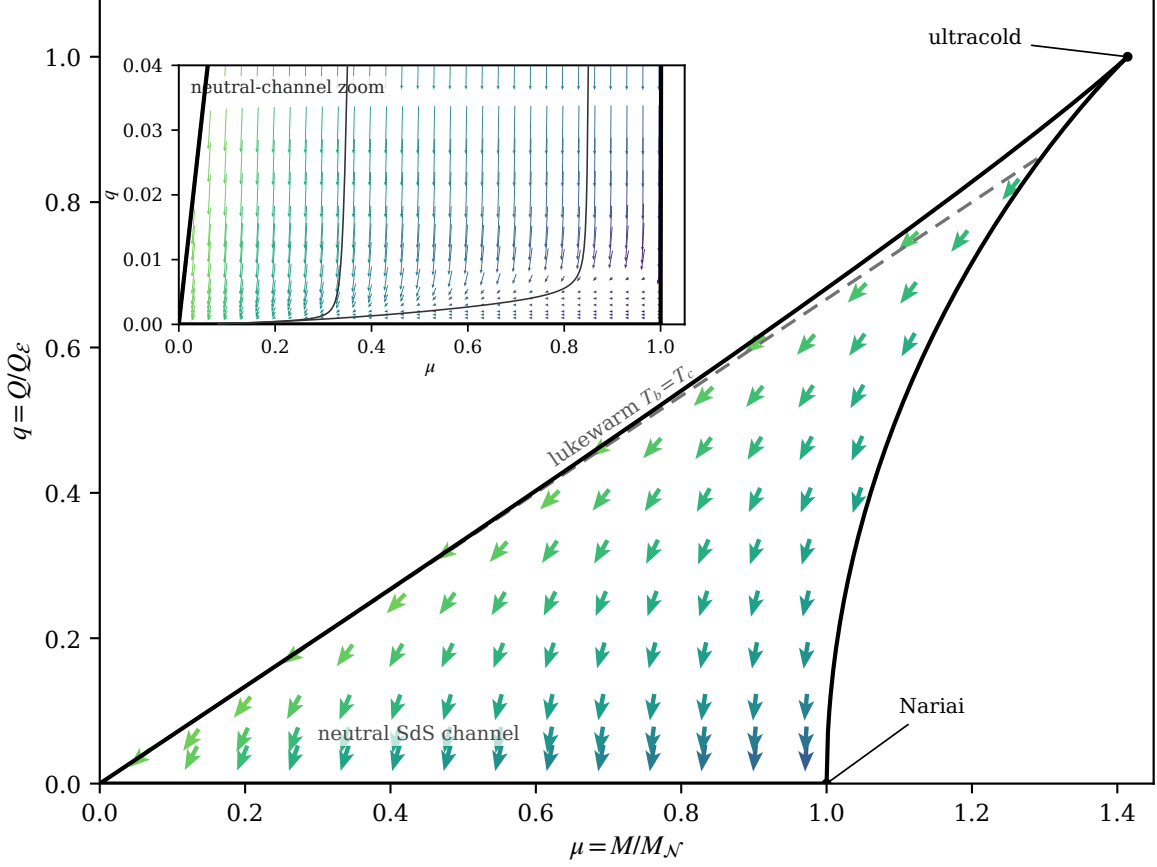


FIG. 1. Semiclassical RN–dS phase portrait in dimensionless variables $(\mu, q) = (M/M_{\mathcal{N}}, Q/Q_{\mathcal{E}})$. The solid black curve is the physical RN–dS double-root boundary: the cold/extremal branch and the charged Nariai branch meet at the ultracold point, while the neutral Nariai point lies at $(\mu, q) = (1, 0)$. The dashed gray line is the classical lukewarm locus $T_b = T_c$, shown only as a reference curve. The arrows show the local vector field computed from the full semiclassical evolution equations, including the electromagnetic work term $\dot{M} = -\mathcal{F} + \Phi_b \dot{Q}$, together with the Schwinger discharge law for \dot{Q} . Colors encode $\log_{10} \sqrt{(d\mu/d\tau)^2 + (dq/d\tau)^2}$, rescaled for visual contrast. The inset zooms into the near-neutral region and shows the turnover into the neutral SdS channel; the thin curves are integrated trajectories of the same full dynamical system.

evolution and show that, under realistic assumptions about the charged matter content, neither lukewarm nor charged Nariai configurations arise as late-time attractors.

E. Quantitative hierarchy of discharge and evaporation timescales

The phase portrait in Fig. 1 is governed by the sign structure (26), while the detailed shape of the trajectories is controlled by the *relative* sizes of the mass-loss and charge-loss rates. In this subsection we provide a quantitative estimate of the corresponding timescales, showing

that Schwinger discharge is parametrically faster than Hawking mass loss for macroscopic black holes in the unsuppressed-discharge regime.

Hawking mass-loss timescale.— The anomaly-induced flux law (16) gives

$$\dot{M}_{\text{H}} = -\frac{N_{\text{eff}}}{48\pi} \left[\kappa_b^2(M, Q) - \kappa_c^2(M, Q) \right].$$

Along the neutral branch ($Q = 0$) we prove in Appendix A that $\kappa_b > \kappa_c$ for all $0 < M < M_{\mathcal{N}}$, implying $\dot{M}_{\text{H}} < 0$. Defining $\Delta\kappa^2 \equiv \kappa_b^2 - \kappa_c^2$, the characteristic mass-loss timescale is

$$t_M \sim \frac{M}{|\dot{M}_{\text{H}}|} \simeq \frac{48\pi M}{N_{\text{eff}} \Delta\kappa^2}.$$

In the small-black-hole regime

$$2G_4M \ll H^{-1}, \quad H = \sqrt{\Lambda/3},$$

one has

$$\kappa_b \simeq \frac{1}{4G_4M}, \quad \kappa_c \sim \mathcal{O}(H).$$

Thus, when $\kappa_b \gg \kappa_c$,

$$\Delta\kappa^2 \simeq \frac{1}{16G_4^2M^2},$$

and the anomaly-induced mass-loss time is

$$t_M \sim \frac{M}{|\dot{M}_{\text{H}}|} \simeq \frac{768\pi G_4^2 M^3}{N_{\text{eff}}},$$

or $t_M \simeq 768\pi M^3/N_{\text{eff}}$ in Planck units. For a solar-mass black hole, $M \simeq 9 \times 10^{37}$ in Planck units, the characteristic anomaly-induced mass-loss time is

$$t_M \simeq \frac{10^{117}}{N_{\text{eff}}} t_{\text{Pl}} \sim \frac{10^{74}}{N_{\text{eff}}} \text{ s}.$$

This is a characteristic instantaneous mass-loss timescale rather than an integrated lifetime.

Schwinger discharge timescale.— The charge-loss law (19) contains the Schwinger exponent

$$\exp\left[-\frac{\pi m_{\text{eff}}^2}{e_{\text{eff}} E_b}\right], \quad E_b = \frac{|Q|}{r_b^2},$$

where E_b is the magnitude of the electric field at the black-hole horizon. For $Q > 0$, define

$$\zeta \equiv \frac{\pi m_{\text{eff}}^2 r_b^2}{e_{\text{eff}} Q}.$$

In the same regime, define the dimensionless charge fraction

$$f \equiv \frac{|Q|}{\sqrt{G_4} M}.$$

Up to corrections of order $H^2 r_b^2$, the black-hole horizon is approximately the Reissner–Nordström value

$$r_b \simeq G_4 M \left(1 + \sqrt{1 - f^2}\right),$$

so in Planck units

$$\zeta \simeq \frac{\pi m_{\text{eff}}^2}{e_{\text{eff}}} M \frac{\left(1 + \sqrt{1 - f^2}\right)^2}{f}.$$

Thus the numerical size of the exponent depends on the charge fraction f . For $f = O(1)$, including near-extremal charge fractions, the exponent is well below unity for stellar-mass black holes when the electron is the dominant available charged species, up to convention-dependent normalizations of the electromagnetic coupling. In the small- f approximation $r_b \simeq 2M$, this reduces to

$$\zeta \simeq \frac{4\pi m_{\text{eff}}^2}{e_{\text{eff}}} \frac{M}{f}.$$

In the unsuppressed regime $\zeta \ll 1$, the Schwinger law (19) reduces, for $Q > 0$, to

$$\dot{Q} \simeq -\bar{\beta}_{\text{Sch}} \ell_* \frac{e_{\text{eff}}^2}{2\pi r_b^2} Q.$$

Thus the charge decays exponentially with e-folding time

$$t_Q = \frac{Q}{|\dot{Q}|} \simeq \frac{2\pi r_b^2}{\bar{\beta}_{\text{Sch}} \ell_* e_{\text{eff}}^2}.$$

For $r_b \simeq 2G_4 M$,

$$t_Q \simeq \frac{8\pi G_4^2 M^2}{\bar{\beta}_{\text{Sch}} \ell_* e_{\text{eff}}^2}.$$

For fixed microscopic ℓ_* , this scales as $t_Q \sim M^2$.

Hierarchy and physical implications.— By contrast, in this regime the anomaly-induced Hawking mass-loss time scales as $t_M \sim M^3$. More explicitly, using $\kappa_b \simeq (4M)^{-1}$ and $\kappa_c \ll \kappa_b$,

$$t_M \simeq \frac{768\pi M^3}{N_{\text{eff}}}.$$

Combining this with the unsuppressed Schwinger estimate $t_Q \simeq 2\pi r_b^2 / (\bar{\beta}_{\text{Sch}} \ell_* e_{\text{eff}}^2)$ in the small-charge geometric approximation $r_b \simeq 2M$, gives

$$\frac{t_Q}{t_M} \simeq \frac{N_{\text{eff}}}{96 \bar{\beta}_{\text{Sch}} e_{\text{eff}}^2} \frac{1}{\ell_* M}.$$

For a microscopic matching length of order the fundamental scale, $\ell_* M \gg 1$ for macroscopic black holes, so $t_Q/t_M \ll 1$ in the unsuppressed-discharge regime. Thus neutralization occurs on a timescale parametrically short compared with Hawking evaporation.²

This is consistent with the worldline-instanton analysis of [22], wherein it was shown that the Schwinger exponent is minimized in the $\text{AdS}_2 \times S^2$ near-horizon region and that contributions from larger radii are exponentially subdominant in their asymptotically flat extremal RN setting. This supports the assumption that the dominant discharge rate is controlled by the near-horizon electric field E_b . Curvature corrections, greybody factors, and matching effects may renormalize the prefactor and the precise range of validity of the horizon-local estimate. Within our effective discharge model, they enter through nonnegative rate or transmission factors, leaving the sign of \dot{Q} unaltered. The rapid-discharge hierarchy persists in the unsuppressed regime as long as the effective prefactor is not parametrically small.

This hierarchy is the quantitative origin of the nearly vertical flow in Fig. 1: trajectories rapidly move toward $q = 0$ before appreciable anomaly-driven Hawking evaporation occurs, while the full mass evolution continues to include the electromagnetic work term $\Phi_b \dot{Q}$. They then evolve slowly along the neutral SdS branch. Consequently, in any theory with an operative discharge channel in the rapid-discharge regime, controlled trajectories proceed through rapid neutralization followed by monotonic Hawking-driven decay along the neutral SdS channel to the empty de Sitter endpoint.

² The Schwinger exponent depends on the charge fraction $f = |Q|/(\sqrt{G_4}M)$. For an electron and a stellar-mass black hole with $f = O(1)$, the RN estimate is convention-dependently of order 10^{-6} – 10^{-4} , well below unity. As $|Q|$ becomes very small the exponent eventually grows, but by then the black hole has already been neutralized for the purposes of the macroscopic phase portrait.

VI. STEADY STATES, EXTREMAL LIMITS, AND PHASE STRUCTURE

Thermal equilibrium of the two outer horizons requires $T_b = T_c$. For neutral SdS this occurs only in the Nariai limit, while in the charged RN–dS family there is a classical lukewarm locus with $T_b = T_c \neq 0$. In addition, the static solution space contains distinguished degenerate boundaries: the cold/extremal branch $r_- = r_b$, the charged Nariai branch $r_b = r_c$, and their ultracold endpoint $r_- = r_b = r_c$. None of these classical loci is a full-flow attractor once semiclassical backreaction and discharge are included.

A. Charged Nariai limit

One boundary of the admissible static-patch region is the charged Nariai curve $r_b = r_c \equiv r_N$, where both surface gravities with respect to the original static-patch Killing time vanish.³ Although \mathcal{F} vanishes identically at these points, exact charged Nariai data are not an attracting endpoint for controlled nondegenerate interior trajectories. Subextremal perturbations that split the double root move the solution into the interior of the admissible static-patch region. Once Schwinger discharge drives $|Q|$ toward zero, the geometry is funneled into a neighborhood of the neutral SdS branch, where the proven inequality $\kappa_b(M, 0) > \kappa_c(M, 0)$ for $0 < M < M_N$ (Appendix A) ensures a net outward flux and continued evaporation.

If charged fields capable of Schwinger production exist, the charged Nariai branch is not an attracting endpoint for the physical interior phase portrait. Formally, away from the ultracold endpoint, the reduced adiabatic energy balance is tangent to the charged Nariai double-root curve. In geometric variables,

$$\mathbf{m} \equiv G_4 M, \quad \mathbf{q} \equiv \sqrt{G_4} Q,$$

the charged Nariai double-root conditions give

$$\mathbf{q}^2 = r_N^2 \left(1 - \frac{3r_N^2}{L^2} \right), \quad \mathbf{m} = r_N \left(1 - \frac{2r_N^2}{L^2} \right).$$

³ This refers to the Killing normalization used in the conserved-current calculation. Observer-normalized Nariai temperatures need not vanish and are the appropriate quantities for local heat-capacity questions.

Hence, away from the ultracold cusp where the parametrization degenerates,

$$\frac{d\mathbf{m}}{d\mathbf{q}} = \frac{\mathbf{q}}{r_N}.$$

On the charged Nariai curve $\mathcal{F} = 0$, and the work term gives

$$\dot{\mathbf{m}} = \frac{\mathbf{q}}{r_N} \dot{\mathbf{q}} = \frac{d\mathbf{m}}{d\mathbf{q}} \dot{\mathbf{q}}.$$

Thus the formal reduced flow is tangent to the double-root boundary, and exact degenerate data require separate treatment. The endpoint statement used here concerns controlled nondegenerate trajectories in the static-patch domain: subextremal perturbations that split the double root move the solution into the interior, where the coupled anomaly-discharge flow drives the system away from the charged equilibrium structure and toward the neutral SdS channel.

B. Extremal RN–dS limit

The cold/extremal curve $\kappa_b = 0$ forms yet another boundary of the Reissner–Nordström–de Sitter family. Classically this corresponds to a degenerate black-hole horizon, but away from the ultracold endpoint the cosmological horizon remains simple with $\kappa_c > 0$. The anomaly-driven flux therefore satisfies $\dot{M}_H \propto +\kappa_c^2 > 0$ along the extremal branch, so the semiclassical evolution drives the system *away* from extremality in the mass direction.

The complementary instability in charge is governed by Schwinger discharge: unless all charged species are absent, \dot{Q}_{Sch} has the opposite sign of Q and the magnitude $|Q|$ decreases. Thus the anomaly-only contribution pushes away from the cold branch in the mass direction, while Schwinger discharge decreases $|Q|$. Consequently, the cold branch is not an attractor of the full flow.

Relation to the Cauchy horizon.— The outer-horizon evolution studied here is logically separate from the inner-horizon problem of strong cosmic censorship. Nevertheless, the two pictures are complementary. Charged type–D geometries that possess inner horizons are susceptible to semiclassical stress-tensor amplification at those horizons [41–46]. The present result addresses a different part of the same problem: in the rapid-discharge regime, the outer adiabatic flow drives the solution toward the neutral SdS channel, so it does not

select a persistent charged RN–dS endpoint with a late-time inner horizon. Thus the phase-space flow and the local Cauchy-horizon instability point in the same direction, while relying on distinct semiclassical mechanisms.

C. Full-flow status of the lukewarm curve

The celebrated lukewarm curve is often interpreted as an equilibrium family because the two outer horizons have equal temperatures. We now show that this is only a fixed-charge anomaly-flux condition, not an invariant condition for the full semiclassical flow.

Let us denote the classical lukewarm locus by

$$\mathcal{L}_{\text{LW}} : \quad \kappa_b(M, Q) = \kappa_c(M, Q). \quad (29)$$

The locus is depicted in Fig. 1 by the dashed gray curve. On \mathcal{L}_{LW} the Polyakov flux (16) vanishes, $\mathcal{F} = 0$. However, the full semiclassical flow also contains the discharge term and the associated electromagnetic work contribution, so $\mathcal{F} = 0$ is not by itself a full-flow equilibrium condition.

For the standard RN–dS family, the $Q > 0$ lukewarm branch is simply

$$\mathfrak{q} = \mathfrak{m},$$

with the $Q < 0$ branch obtained by charge conjugation. On the lukewarm locus $\mathcal{F} = 0$, so the mass evolution equation gives

$$\dot{\mathfrak{m}} = \varphi_b \dot{\mathfrak{q}}, \quad \varphi_b \equiv \frac{\mathfrak{q}}{r_b}.$$

Hence

$$\frac{d}{dv}(\mathfrak{m} - \mathfrak{q}) = (\varphi_b - 1)\dot{\mathfrak{q}}.$$

Along the subextremal lukewarm branch one has

$$r_b > \mathfrak{q} = \mathfrak{m},$$

and therefore $0 < \varphi_b < 1$. Since Schwinger discharge gives $\dot{\mathbf{q}} < 0$, it follows that

$$\frac{d}{dv}(\mathbf{m} - \mathbf{q}) > 0.$$

Thus the full semiclassical vector field is not tangent to the lukewarm curve: even exactly lukewarm initial data immediately leave the lukewarm locus once discharge is operative.

Equivalently, the lukewarm curve is only the nullcline of the Polyakov heat flux, not a full-flow mass nullcline. It cannot be a dynamical attractor of the coupled semiclassical system unless all charged species are kinematically inaccessible. This is the only stability statement needed for the endpoint argument; no assumption about attraction along the fixed-charge anomaly-flow nullcline is made. Combining these observations gives the part of the phase portrait needed for our endpoint theorem. The cold/extremal curve is not an attracting invariant set, the charged Nariai boundary is not an attracting endpoint for controlled nondegenerate interior trajectories, and the lukewarm locus is left in the charge direction once Schwinger discharge is active. Thus controlled rapid-discharge trajectories waterfall toward the neutral line (see inset in Fig. 1), where Appendix A guarantees monotonic mass loss along the $Q = 0$ channel.

VII. END STATES AND NO-REMNANT RESULT

We now formulate the *no-remnant consequence* of the phase portrait described above. The result applies to controlled nondegenerate trajectories in the static-patch domain whenever an operative Schwinger discharge channel exists. In this rapid-discharge regime, the semiclassical flow carries charged data toward the neutral SdS channel, where $\kappa_b(M, 0) > \kappa_c(M, 0)$ enforces continued mass loss. Thus the classical distinguished loci of the RN–dS family cannot be selected as late-time remnants by the coupled anomaly-discharge evolution. The limit $M \rightarrow 0$ should be understood as the formal endpoint of the adiabatic semiclassical evolution; possible Planck-scale corrections near $M \sim M_{\text{Pl}}$ lie outside the regime of control.

Theorem 1 (Global semiclassical endpoint). *Let (M_0, Q_0) be sub-Nariai initial data whose adiabatic trajectory remains in the RN–dS static-patch domain during the rapid-discharge stage. Suppose that at least one charged species provides an operative Schwinger discharge channel with $t_Q \ll t_M$ until the charge is macroscopically negligible. Within the anomaly-*

induced semiclassical description governed by Eqs. (24)–(25), the controlled nondegenerate flow selects the formal endpoint

$$(M, Q) = (0, 0).$$

Thus the late-time endpoint in this approximation is empty de Sitter space, rather than an extremal, lukewarm, or charged/neutral Nariai remnant.

Proof. For $Q \neq 0$, the Schwinger term satisfies

$$\text{sgn}(Q)\dot{Q}_{\text{Sch}} < 0,$$

so $|Q|$ decreases monotonically. In the unsuppressed regime the discharge time satisfies $t_Q \ll t_M$ for macroscopic black holes, so controlled trajectories are rapidly driven into an effectively neutral neighborhood of $Q = 0$, up to the exponentially slow terminal Schwinger tail.

Once the charge is macroscopically negligible, the evolution is governed by the neutral SdS channel. Appendix A proves

$$\kappa_b(M, 0) > \kappa_c(M, 0), \quad 0 < M < M_{\mathcal{N}},$$

and hence

$$\dot{M}_{\text{H}} = -\frac{N_{\text{eff}}}{48\pi} [\kappa_b^2(M, 0) - \kappa_c^2(M, 0)] < 0.$$

Thus the mass decreases monotonically along the neutral branch toward the formal adiabatic endpoint $M \rightarrow 0$.

The cold/extremal curve, the charged Nariai boundary, and the lukewarm curve are not attracting endpoints for controlled nondegenerate trajectories, as shown in Sec. VI. Therefore, within the formal adiabatic continuum description, the controlled semiclassical endpoint is

$$M(v) \rightarrow 0, \quad Q(v) \rightarrow 0,$$

corresponding to empty de Sitter space. □

Corollary 1 (Absence of semiclassical remnants). *No finite-mass, charged, or neutral remnants form under the assumptions of Theorem 1. In particular, extremal RN–dS and charged*

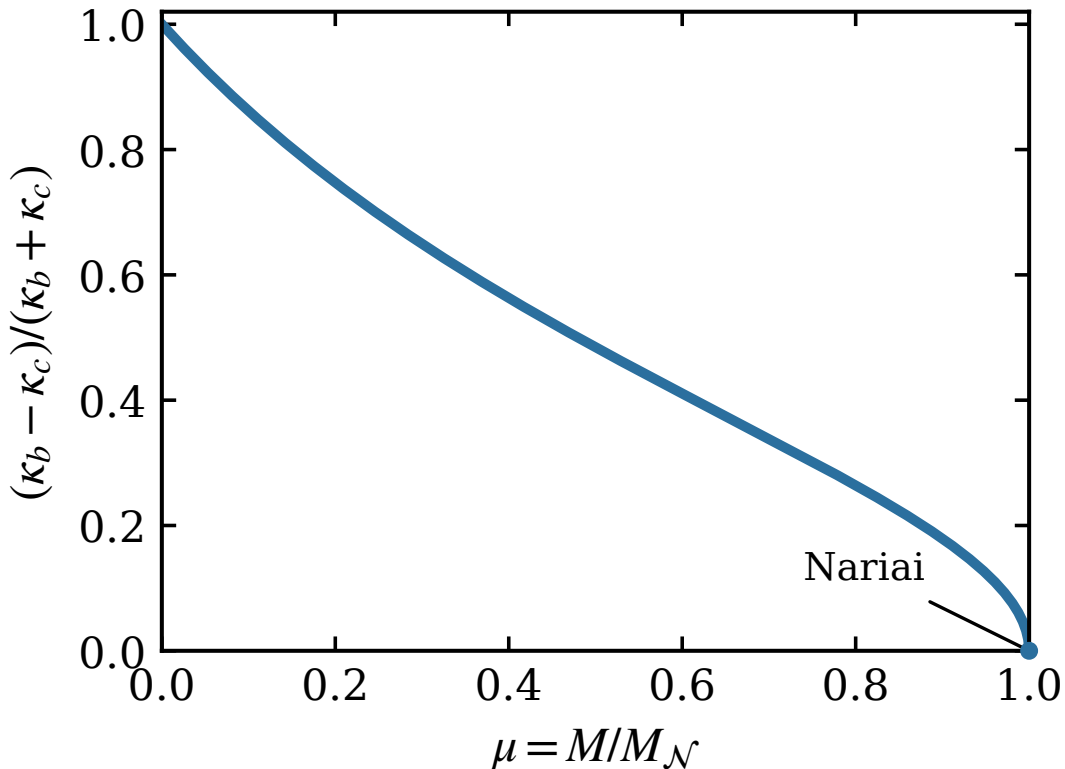


FIG. 2. Relative surface-gravity difference along the neutral Schwarzschild–de Sitter branch, $(\kappa_b - \kappa_c)/(\kappa_b + \kappa_c)$, plotted as a function of $\mu \equiv M/M_N$. The curve remains strictly positive for all $0 < \mu < 1$, showing that the black-hole horizon has larger Killing temperature than the cosmological horizon throughout the sub-Nariai neutral family. The relative difference vanishes only in the Nariai limit, $\mu = 1$, where $\kappa_b = \kappa_c = 0$. This numerically illustrates the analytic ordering $\kappa_b > \kappa_c$ proved in Appendix A, which implies $\kappa_b^2 - \kappa_c^2 > 0$ and hence monotonic anomaly-driven mass loss along the neutral SdS channel.

or neutral Nariai geometries cannot be semiclassical endpoints for controlled nondegenerate rapid-discharge trajectories.

VIII. INFORMATION-THEORETIC INTERPRETATION

The same two-dimensional semiclassical framework provides the natural input for an island estimate of the radiation entropy. Here, we do not attempt a microscopic derivation of the exact fine-grained Page curve for RN–dS evaporation. Such formidable derivation would require specifying the radiation region, the global quantum state, the UV subtraction convention in S_{out} , and the fully time-dependent QES geometry. We do, however, extract the robust semiclassical consequence of the dynamical solution: the background entering

the island problem is driven rapidly toward the neutral SdS channel whenever Schwinger discharge is operative.

Island constructions in cosmological and de Sitter settings have been studied in several complementary models [27–30]; we take these as motivation for a conservative saddle-competition estimate on the dynamically selected RN–dS background.

The generalized entropy of an island endpoint is

$$S_{\text{gen}}[\partial\mathcal{I}] = \frac{A(\partial\mathcal{I})}{4G_4} + S_{\text{out}}(\mathcal{R} \cup \mathcal{I}),$$

or equivalently, in the two-dimensional reduction, $A = 4\pi X$. The fine-grained radiation entropy is estimated by the usual competition between the no-island and island saddles [24–26],

$$S_{\text{fine}}(v) = \min\{S_{\text{no island}}(v), S_{\text{island}}(v)\}.$$

In the adiabatic Unruh–dS state, the no-island branch is controlled by the accumulated Hawking entropy in the static patch, while the island branch is dominated by the area term evaluated at a QES exponentially close to the black-hole horizon,

$$S_{\text{island}}(v) \simeq \frac{A_b(v)}{4G_4} + O(N_{\text{eff}}) = \frac{\pi r_b(v)^2}{G_4} + O(N_{\text{eff}}).$$

The Page time is therefore estimated by the branch-crossing condition

$$S_{\text{no island}}(v_{\text{Page}}) \simeq S_{\text{island}}(v_{\text{Page}}).$$

Within the present adiabatic approximation, charge affects this estimate through the time-dependent background $r_b(M(v), Q(v))$, $\kappa_b(M(v), Q(v))$, and $\kappa_c(M(v), Q(v))$. In the rapid-discharge regime studied above, $t_Q \ll t_M$, so $Q(v)$ becomes negligible long before the mass changes appreciably. The subsequent island problem is therefore a smooth deformation of the neutral SdS problem and quickly reduces to the neutral channel. Thus the phase portrait not only fixes the semiclassical endpoint but also identifies the background on which the late-time QES competition is to be evaluated.

Since the Page estimate is controlled by the slow Hawking evolution, while the discharge time satisfies $t_Q \ll t_M$ in the macroscopic unsuppressed-discharge regime, charge-dependent

corrections to the late-time island saddle are parametrically transient. The geometry has already become effectively neutral by the time the no-island and island branches compete. Thus the charged problem does not require a new late-time QES mechanism: the relevant saddle competition reduces to the neutral SdS channel, with only early-time charge-dependent corrections during the discharge stage.

Should discharge be kinematically forbidden, the same formalism results instead in a fixed-charge anomaly-flow problem. In that nongeneric regime the geometry may approach the anomaly-flux equilibrium locus rather than the neutral evaporation channel, and the corresponding entropy history is appropriately analyzed on that fixed-charge background rather than inferred from the rapid-discharge case. A full calculation of the fixed-charge QES geometry lies beyond the scope of this work.

IX. CONCLUSIONS

We have developed an analytic semiclassical model for the nonequilibrium discharge and evaporation of Reissner–Nordström–de Sitter black holes within the spherically symmetric, anomaly-induced adiabatic approximation. The Polyakov sector fixes a conserved horizon-to-horizon Killing-energy flux proportional to $\kappa_b^2 - \kappa_c^2$, while the full mass evolution includes the electromagnetic work term associated with charge loss. Together with a near-horizon Schwinger discharge law, this gives a closed evolution system for the mass and charge of the black hole.

The main result is a two-stage endpoint paradigm. In the rapid-discharge regime, any active sufficiently light charged species drives the system toward the neutral line on a timescale parametrically shorter than the anomaly-induced Hawking mass-loss time. Once the trajectory reaches an effectively neutral neighborhood, the neutral SdS ordering proved in Appendix A fixes the sign of the remaining Hawking evolution and implies monotonic mass loss. Controlled rapid-discharge trajectories therefore select the formal adiabatic endpoint $(M, Q) = (0, 0)$, corresponding to empty de Sitter space.

This endpoint does not follow by assuming a global temperature ordering in the charged RN–dS family. The charged solution space contains the lukewarm locus $T_b = T_c$, where the anomaly-induced heat flux vanishes. The crucial point is dynamical: the lukewarm curve is only a nullcline of the Polyakov flux, not an invariant locus or mass nullcline of the full

anomaly-discharge flow. Similarly, the cold/extremal branch, charged Nariai branch, and ultracold point are distinguished classical loci, but they are not attracting endpoints when charge loss is dynamically active. The nonequilibrium dynamics reorganizes the classical phase diagram: charge is shed first, and the neutral SdS evaporation channel determines the endpoint.

The same framework gives a controlled thermodynamic interpretation. The anomaly-mediated heat flow satisfies the coarse-grained horizon generalized second law in the static patch, while the time-dependent background supplies the appropriate semiclassical geometry for island/QES estimates. In the rapid-discharge regime, the charge-dependent part of the geometry is transient on the timescale relevant for late-time saddle competition, so the information-theoretic estimate reduces smoothly to the neutral SdS channel.

Our framework has a precise domain of validity: spherical symmetry, the Polyakov anomaly sector for conformal s-wave matter, an adiabatic Unruh–de Sitter state, and a near-horizon effective description of Schwinger discharge. Greybody factors, dilaton-dependent anomaly terms, higher-derivative corrections, and finite- N effects can modify coefficients and state-dependent details. However, within any regime in which the neutral flux retains the sign fixed by $\kappa_b > \kappa_c$ and discharge remains faster than mass loss, these corrections are not expected to change the endpoint mechanism. Naturally, Planck-scale physics near the formal endpoint lies outside the regime of control.

More broadly, the RN–dS system suggests a general endpoint principle for charged multi-horizon spacetimes: when a conserved horizon-to-horizon energy current is combined with a fast discharge channel, charged equilibrium loci need not control the late-time fate. Instead, the neutral surface-gravity ordering can act as the endpoint selector. Testing this principle beyond spherical symmetry, including slow rotation, greybody-resolved fluxes, and more general anomaly sectors, is a fruitful direction for future work.

ACKNOWLEDGMENTS

It is a pleasure to thank Lars Aalsma, Paul Davies and Tanmay Vachaspati for useful discussions. This work is supported by the U.S. Department of Energy, Office of High Energy Physics, under Award Number DE-SC0019470.

Appendix A: Ordering of Horizon Surface Gravities in Sub-Nariai SdS

This appendix provides the mathematical lemma used in Sec. VII: for every neutral Schwarzschild–de Sitter geometry with $0 < M < M_{\mathcal{N}}$, the black-hole horizon has larger Killing surface gravity, equivalently larger Killing temperature in the normalization used here, $\kappa_b > \kappa_c$. The inequality fixes the sign of the anomaly-induced mass change $\dot{M}_{\text{H}} = -\mathcal{F}$ along the neutral line of the (M, Q) phase portrait and thereby guarantees monotonic mass loss toward $M \rightarrow 0$. We now provide a brief and rigorous proof of the inequality.

1. Setup and notation

For $0 < M < M_{\mathcal{N}}$, the metric function

$$f(r) = 1 - \frac{2G_4 M}{r} - \frac{\Lambda r^2}{3}$$

admits three real roots,

$$r_0 < 0 < r_b < r_c,$$

corresponding to the unphysical negative root r_0 , the black-hole horizon r_b , and the cosmological horizon r_c .

In Sec. II we showed that the surface gravities can be written in the closed forms

$$\kappa_b = \frac{(r_c - r_b)(2r_b + r_c)}{2r_b(r_b^2 + r_b r_c + r_c^2)}, \quad (\text{A1})$$

$$\kappa_c = \frac{(r_c - r_b)(r_b + 2r_c)}{2r_c(r_b^2 + r_b r_c + r_c^2)}. \quad (\text{A2})$$

These expressions follow directly from the factorization

$$f(r) = -\frac{\Lambda}{3r}(r - r_b)(r - r_c)(r - r_0)$$

together with $\kappa_i = \frac{1}{2}|f'(r_i)|$, and may be taken as equivalent to the corresponding surface-gravity formulas in the main text.

2. Proof of $\kappa_b > \kappa_c$

In the sub-Nariai regime the following quantities are manifestly positive:

$$r_c - r_b > 0, \quad r_b > 0, \quad r_c > 0, \quad r_b^2 + r_b r_c + r_c^2 > 0.$$

Thus both κ_b and κ_c are strictly positive.

To compare them, factor out the positive constant

$$C \equiv \frac{r_c - r_b}{2(r_b^2 + r_b r_c + r_c^2)} > 0.$$

Then (A1)–(A2) take the form

$$\kappa_b = C \frac{2r_b + r_c}{r_b}, \tag{A3}$$

$$\kappa_c = C \frac{r_b + 2r_c}{r_c}. \tag{A4}$$

Since $C > 0$, the inequality $\kappa_b > \kappa_c$ is equivalent to

$$\frac{2r_b + r_c}{r_b} > \frac{r_b + 2r_c}{r_c}. \tag{A5}$$

Rewrite both sides:

$$\frac{2r_b + r_c}{r_b} = 2 + \frac{r_c}{r_b}, \quad \frac{r_b + 2r_c}{r_c} = 2 + \frac{r_b}{r_c}.$$

Subtracting 2 from (A5) yields the equivalent inequality

$$\frac{r_c}{r_b} > \frac{r_b}{r_c}.$$

Let $x \equiv r_c/r_b$. In the sub-Nariai region one has $r_c > r_b > 0$, hence $x > 1$. The inequality becomes

$$x > \frac{1}{x}.$$

Multiplying by $x > 0$,

$$x^2 > 1,$$

which is clearly true for all $x > 1$. This establishes the result:

$$\kappa_b > \kappa_c > 0 \quad \text{for all } 0 < r_b < r_c.$$

3. Nariai limit

As $r_b \rightarrow r_c$, the common prefactor C tends to zero and both surface gravities vanish:

$$\kappa_b \rightarrow 0, \quad \kappa_c \rightarrow 0.$$

Thus the Nariai spacetime is the unique double-zero of the surface gravities. It is a zero-flux boundary configuration, but not a stable endpoint: perturbations that split the horizons restore the neutral ordering $\kappa_b > \kappa_c$ and restart evaporation.

4. Implication for semiclassical evolution

Since $\kappa_b > \kappa_c$ for all $0 < M < M_{\mathcal{N}}$, the anomaly flux satisfies $\mathcal{F}(M, 0) > 0$, equivalently $\dot{M}_{\text{H}}(M, 0) = -\mathcal{F}(M, 0) < 0$, on the entire interval, so the neutral mass decreases monotonically to $M \rightarrow 0$. The Nariai point ($\kappa_b = \kappa_c = 0$) is a static solution at the upper mass bound. Although radiation from the cosmological horizon provides an external influx, it is always subdominant to the black-hole outflow for $M < M_{\mathcal{N}}$, so the Nariai configuration is not approached dynamically from the sub-Nariai neutral branch by Hawking evaporation.

Appendix B: Conserved Killing current and Polyakov flux

This appendix verifies two ingredients used in the main text in the presence of charge: (i) the existence of a radially conserved Killing-energy current in the static patch, and (ii) the resulting appearance of the combination $\kappa_b^2 - \kappa_c^2$ in the *Polyakov* (pure conformal) contribution to the net horizon-to-horizon flux. The derivation is the same as in the neutral SdS case, by simply replacing $\xi(r)$ by $\xi(r; M, Q)$.

1. Static patch and a conserved flux

In the static region $r_b < r < r_c$, the four-dimensional RN–dS metric is

$$ds^2 = -\xi(r) dt^2 + \xi(r)^{-1} dr^2 + r^2 d\Omega_2^2, \quad \xi(r) = 1 - \frac{2G_4 M}{r} + \frac{G_4 Q^2}{r^2} - \frac{\Lambda r^2}{3}, \quad (\text{B1})$$

with $\xi(r_b) = \xi(r_c) = 0$ and $0 < r_b < r_c$. Introduce the tortoise coordinate $dr_*/dr = \xi^{-1}$ and null coordinates

$$u = t - r_*, \quad v = t + r_*, \quad (\text{B2})$$

so the reduced two-dimensional line element takes the conformal form

$$ds_2^2 = -\xi(r) du dv. \quad (\text{B3})$$

Let T_{ab} be a symmetric, stationary, covariantly conserved two-dimensional stress tensor

$$\nabla_a T^{ab} = 0, \quad (\text{B4})$$

in particular the anomaly-induced expectation value obtained from the Polyakov action. The static Killing vector $\zeta^a = (\partial_t)^a$ defines the Killing-energy current

$$J^a \equiv -T^a{}_b \zeta^b. \quad (\text{B5})$$

Using $\nabla_{(a} \zeta_{b)} = 0$ and (B4),

$$\nabla_a J^a = -(\nabla_a T^a{}_b) \zeta^b - T^{ab} \nabla_a \zeta_b = 0. \quad (\text{B6})$$

In the (t, r) coordinates of (B1), $\sqrt{-g_{(2)}} = 1$, so (B6) implies

$$\partial_r J^r = 0 \quad \Rightarrow \quad \partial_r (T^r{}_t) = 0, \quad (\text{B7})$$

since $J^r = -T^r{}_t$ for $\zeta = \partial_t$. Thus the mixed component $T^r{}_t$ is *radially constant* throughout the static patch.

In the null coordinates (B2) one has the identity

$$T^r_t = T_{vv} - T_{uu}, \quad (\text{B8})$$

so we define the conserved mixed component

$$\mathcal{I} \equiv T^r_t = T_{vv} - T_{uu}, \quad \Rightarrow \quad \partial_r \mathcal{I} = 0. \quad (\text{B9})$$

This \mathcal{I} is the signed mixed stress-tensor component. The positive outward flux used in the main text is defined with the opposite sign when the black-hole horizon is hotter: $\mathcal{F}_P \equiv -\mathcal{I}$.

2. Horizon regularity and universal Schwarzian offsets

Let r_h be any *simple* Killing horizon of $\xi(r)$, with surface gravity

$$\kappa_h \equiv \frac{1}{2} |\xi'(r_h)|. \quad (\text{B10})$$

Define future-horizon affine Kruskal coordinates separately in each chiral sector:

$$U_h = -e^{-\kappa_h u} \quad (\text{outgoing sector}), \quad V_h = -e^{-\kappa_h v} \quad (\text{ingoing sector}). \quad (\text{B11})$$

For the pure conformal (Polyakov) sector with central charge $c = N$, the chiral components obey the projective (Schwarzian) transformation law

$$\langle T_{uu} \rangle = \left(\frac{dU_h}{du} \right)^2 \langle T_{U_h U_h} \rangle - \frac{N}{24\pi} \{U_h, u\}, \quad (\text{B12})$$

$$\langle T_{vv} \rangle = \left(\frac{dV_h}{dv} \right)^2 \langle T_{V_h V_h} \rangle - \frac{N}{24\pi} \{V_h, v\}, \quad (\text{B13})$$

where $\{\cdot, \cdot\}$ is the Schwarzian derivative. For the exponential maps in (B11) one has

$$\{U_h, u\} = \{V_h, v\} = -\frac{1}{2} \kappa_h^2. \quad (\text{B14})$$

In the static Polyakov solution the chiral components may be written as

$$\langle T_{uu} \rangle = B(r) + t_u, \quad \langle T_{vv} \rangle = B(r) + t_v,$$

where $B(r)$ is the common state-independent geometric term and t_u, t_v are state-dependent chiral constants. With the standard Polyakov normalization,

$$B(r_h) = -\Theta_h, \quad \Theta_h \equiv \frac{N}{48\pi} \kappa_h^2. \quad (\text{B15})$$

Near a simple horizon, an affine Kruskal coordinate in the outgoing sector may be taken as $U_h = -e^{-\kappa_h u}$. Since

$$\langle T_{U_h U_h} \rangle = \left(\frac{du}{dU_h} \right)^2 \langle T_{uu} \rangle,$$

finiteness of $\langle T_{U_h U_h} \rangle$ at $U_h = 0$ requires

$$\langle T_{uu} \rangle = O(U_h^2).$$

Thus the leading horizon value must vanish,

$$B(r_h) + t_u = 0,$$

and outgoing regularity at r_h fixes

$$t_u = \Theta_h.$$

Similarly, ingoing regularity in an affine coordinate $V_h = -e^{-\kappa_h v}$ fixes

$$t_v = \Theta_h.$$

3. Two-horizon outer prescription and the $(\kappa_b^2 - \kappa_c^2)$ combination

In the RN–dS static patch the relevant outer horizons are the black-hole horizon r_b and the cosmological horizon r_c . The “two-horizon” outer prescription used in the main text is:

- impose *outgoing* affine regularity on the future black-hole horizon \mathcal{H}_b^+ , so $t_u = \Theta_b$;
- impose *ingoing* affine regularity on the future cosmological horizon \mathcal{H}_c^+ , so $t_v = \Theta_c$.

Equivalently,

$$t_u = \Theta_b = \frac{N}{48\pi} \kappa_b^2, \quad t_v = \Theta_c = \frac{N}{48\pi} \kappa_c^2, \quad (\text{B16})$$

where $\kappa_{b,c} = \frac{1}{2} |\xi'(r_{b,c})|$ are defined by (B10) for the charged $\xi(r; M, Q)$.

Since the common term $B(r)$ cancels,

$$\mathcal{I} = T_{vv} - T_{uu} = t_v - t_u \quad (\text{B17})$$

is radially conserved. Using Eq. (B16), one obtains

$$\mathcal{I} = \Theta_c - \Theta_b = -\frac{N}{48\pi} (\kappa_b^2 - \kappa_c^2), \quad (\text{B18})$$

$$\mathcal{F}_P \equiv -\mathcal{I} = \frac{N}{48\pi} (\kappa_b^2 - \kappa_c^2). \quad (\text{B19})$$

4. Adiabatic evolution and first-law energy balance with discharge

Equation (B19) is derived for a fixed static patch. In the large- N /adiabatic regime used in the main text, the evolution is quasistatic: at each advanced time v the geometry is well-approximated by a static RN-dS patch with parameters $(M(v), Q(v))$, so (B19) applies instantaneously with $\kappa_{b,c} = \kappa_{b,c}(M(v), Q(v))$.

When $Q(v)$ changes due to Schwinger discharge, the *total* mass evolution includes the electromagnetic work term. The Polyakov sector fixes the outward-oriented signed flux. In the pure two-dimensional theory this is \mathcal{F}_P in (B19); in the four-dimensional matched evolution we replace N by N_{eff} and denote the result by \mathcal{F} . The first-law energy balance then yields

$$\dot{M} = -\mathcal{F} + \Phi_b \dot{Q}, \quad \Phi_b = \frac{Q}{r_b}, \quad (\text{B20})$$

as used in Eq. (17) of the main text.

5. Remark on additional anomaly terms

If dilaton-dependent anomaly terms are included, as can occur for spherically reduced four-dimensional matter, the horizon regularity offsets need not be the pure Polyakov values $\Theta_h = N\kappa_h^2/(48\pi)$. They can be shifted by additional horizon-local terms depending on

the dilaton and its derivatives. The conserved-current argument nevertheless remains valid: for any covariantly conserved, stationary semiclassical stress tensor on the static patch, $T^r_t = T_{vv} - T_{uu}$ is radially constant. Imposing the same two-horizon regularity prescription therefore gives a difference-of-offsets structure

$$\mathcal{I} = \Theta_c^{\text{tot}} - \Theta_b^{\text{tot}}, \quad \mathcal{F} = \Theta_b^{\text{tot}} - \Theta_c^{\text{tot}}.$$

In the pure Polyakov sector,

$$\Theta_h^{\text{tot}} = \Theta_h = \frac{N}{48\pi} \kappa_h^2,$$

and this reduces to Eq. (B19).

-
- [1] R. Gregory, I. G. Moss, N. Oshita, and S. Patrick, Black hole evaporation in de Sitter space, *Class. Quant. Grav.* **38**, 185005 (2021), [arXiv:2103.09862 \[gr-qc\]](#).
 - [2] L. Aalsma, M. Parikh, and J. P. Van Der Schaar, Back(reaction) to the Future in the Unruh-de Sitter State, *JHEP* **11**, 136, [arXiv:1905.02714 \[hep-th\]](#).
 - [3] D. A. Easson, Fate of Schwarzschild–de Sitter black holes: Nonequilibrium evaporation, *Phys. Rev. D* **113**, 084014 (2026), [arXiv:2511.11873 \[hep-th\]](#).
 - [4] X. Shi, G. J. Turiaci, and C.-H. Wu, The Fate of Nucleated Black Holes in de Sitter Quantum Gravity (2026), [arXiv:2605.03015 \[hep-th\]](#).
 - [5] R. Bousso and S. W. Hawking, (Anti)evaporation of Schwarzschild-de Sitter black holes, *Phys. Rev. D* **57**, 2436 (1998), [arXiv:hep-th/9709224](#).
 - [6] A. M. Polyakov, Quantum Geometry of Bosonic Strings, *Phys. Lett. B* **103**, 207 (1981).
 - [7] P. H. Ginsparg and M. J. Perry, Semiclassical Perdurance of de Sitter Space, *Nucl. Phys. B* **222**, 245 (1983).
 - [8] L. J. Romans, Supersymmetric, cold and lukewarm black holes in cosmological einstein-maxwell theory, *Nucl. Phys. B* **383**, 395 (1992), [arXiv:hep-th/9203018](#).
 - [9] R. Bousso and S. W. Hawking, Pair creation of black holes during inflation, *Phys. Rev. D* **54**, 6312 (1996), [arXiv:gr-qc/9606052](#).
 - [10] A. Castro, F. Mariani, and C. Toldo, Near-extremal limits of de sitter black holes, *JHEP* **07**, 131, [arXiv:2212.14356 \[hep-th\]](#).

- [11] G. W. Gibbons, Vacuum polarization and the spontaneous loss of charge by black holes, *Commun. Math. Phys.* **44**, 245 (1975).
- [12] W. A. Hiscock and L. D. Weems, Evolution of charged evaporating black holes, *Phys. Rev. D* **41**, 1142 (1990).
- [13] G. W. Gibbons and R. E. Kallosh, Topology, entropy and Witten index of dilaton black holes, *Phys. Rev. D* **51**, 2839 (1995), [arXiv:hep-th/9407118](#).
- [14] S. P. Kim and D. N. Page, Schwinger Pair Production in dS(2) and AdS(2), *Phys. Rev. D* **78**, 103517 (2008), [arXiv:0803.2555 \[hep-th\]](#).
- [15] R.-G. Cai and S. P. Kim, One-Loop Effective Action and Schwinger Effect in (Anti-) de Sitter Space, *JHEP* **09**, 072, [arXiv:1407.4569 \[hep-th\]](#).
- [16] R. B. Mann and S. F. Ross, Cosmological production of charged black hole pairs, *Phys. Rev. D* **52**, 2254 (1995), [arXiv:gr-qc/9504015](#).
- [17] B. B. Wang and C. G. Huang, Thermodynamics of reissner–nordstrom–de sitter black hole in york’s formalism, *Class. Quant. Grav.* **19**, 2491 (2002).
- [18] E. K. Morvan, J. P. van der Schaar, and M. R. Visser, Action, entropy and pair creation rate of charged black holes in de Sitter space, *JHEP* **08**, 207, [arXiv:2212.12713 \[hep-th\]](#).
- [19] L. Aalsma, P. Lin, J. P. van der Schaar, G. Shiu, and W. Sybesma, Limits on the Statistical Description of Charged de Sitter Black Holes (2025), [arXiv:2511.03867 \[hep-th\]](#).
- [20] M. Montero, T. Van Riet, and V. Venken, Festina Lente: EFT Constraints from Charged Black Hole Evaporation in de Sitter, *JHEP* **01**, 039, [arXiv:1910.01648 \[hep-th\]](#).
- [21] A. Bhattacharjee and M. Saha, Quantum evolution of de Sitter black holes near extremality, *JHEP* **04**, 129, [arXiv:2510.18035 \[hep-th\]](#).
- [22] P. Lin and G. Shiu, Schwinger effect of extremal Reissner-Nordström black holes, *JHEP* **06**, 017, [arXiv:2409.02197 \[hep-th\]](#).
- [23] L. Aalsma, J. P. van der Schaar, and M. R. Visser, Extremal black hole decay in de Sitter space, *JHEP* **07**, 259, [arXiv:2311.13742 \[hep-th\]](#).
- [24] A. Almheiri, N. Engelhardt, D. Marolf, and H. Maxfield, The entropy of bulk quantum fields and the entanglement wedge of an evaporating black hole, *JHEP* **12**, 063, [arXiv:1905.08762 \[hep-th\]](#).
- [25] G. Penington, Entanglement Wedge Reconstruction and the Information Paradox, *JHEP* **09**, 002, [arXiv:1905.08255 \[hep-th\]](#).

- [26] A. Almheiri, T. Hartman, J. Maldacena, E. Shaghoulian, and A. Tajdini, The entropy of Hawking radiation, *Rev. Mod. Phys.* **93**, 035002 (2021), [arXiv:2006.06872 \[hep-th\]](#).
- [27] T. Hartman, Y. Jiang, and E. Shaghoulian, Islands in cosmology, *JHEP* **11**, 111, [arXiv:2008.01022 \[hep-th\]](#).
- [28] L. Aalsma and W. Sybesma, The Price of Curiosity: Information Recovery in de Sitter Space, *JHEP* **05**, 291, [arXiv:2104.00006 \[hep-th\]](#).
- [29] E. Shaghoulian and L. Susskind, Entanglement in De Sitter space, *JHEP* **08**, 198, [arXiv:2201.03603 \[hep-th\]](#).
- [30] H. Geng, Y. Nomura, and H.-Y. Sun, Information paradox and its resolution in de Sitter holography, *Phys. Rev. D* **103**, 126004 (2021), [arXiv:2103.07477 \[hep-th\]](#).
- [31] D. Grumiller, W. Kummer, and D. V. Vassilevich, Dilaton gravity in two-dimensions, *Phys. Rept.* **369**, 327 (2002), [arXiv:hep-th/0204253](#).
- [32] R. B. Mann, A. Shiekh, and L. Tarasov, Classical and Quantum Properties of Two-dimensional Black Holes, *Nucl. Phys. B* **341**, 134 (1990).
- [33] T. Klosch and T. Strobl, Classical and quantum gravity in (1+1)-Dimensions. Part 1: A Unifying approach, *Class. Quant. Grav.* **13**, 965 (1996), [Erratum: *Class. Quant. Grav.* **14**, 825 (1997)], [arXiv:gr-qc/9508020](#).
- [34] R. Bousso and S. W. Hawking, Trace anomaly of dilaton coupled scalars in two-dimensions, *Phys. Rev. D* **56**, 7788 (1997), [arXiv:hep-th/9705236](#).
- [35] W. Kummer, H. Liebl, and D. V. Vassilevich, Comment on: ‘Trace anomaly of dilaton coupled scalars in two-dimensions’, *Phys. Rev. D* **58**, 108501 (1998), [arXiv:hep-th/9801122](#).
- [36] A. Fabbri, S. Farese, and J. Navarro-Salas, Generalized Virasoro anomaly and stress tensor for dilaton coupled theories, *Phys. Lett. B* **574**, 309 (2003), [arXiv:hep-th/0309160](#).
- [37] S. M. Christensen and S. A. Fulling, Trace Anomalies and the Hawking Effect, *Phys. Rev. D* **15**, 2088 (1977).
- [38] P. C. W. Davies, S. A. Fulling, and W. G. Unruh, Energy Momentum Tensor Near an Evaporating Black Hole, *Phys. Rev. D* **13**, 2720 (1976).
- [39] N. D. Birrell and P. C. W. Davies, *Quantum Fields in Curved Space*, Cambridge Monographs on Mathematical Physics (Cambridge University Press, Cambridge, UK, 1982).
- [40] J. S. Schwinger, On gauge invariance and vacuum polarization, *Phys. Rev.* **82**, 664 (1951).
- [41] E. Poisson and W. Israel, Internal structure of black holes, *Phys. Rev. D* **41**, 1796 (1990).

- [42] A. Ori, Inner structure of a charged black hole: An exact mass-inflation solution, *Phys. Rev. Lett.* **67**, 789 (1991).
- [43] S. Hollands, R. M. Wald, and J. Zahn, Quantum instability of the Cauchy horizon in Reissner–Nordström–deSitter spacetime, *Class. Quant. Grav.* **37**, 115009 (2020), [arXiv:1912.06047](#) [gr-qc].
- [44] S. Hollands, C. Klein, and J. Zahn, Quantum stress tensor at the Cauchy horizon of the Reissner–Nordström–de Sitter spacetime, *Phys. Rev. D* **102**, 085004 (2020), [arXiv:2006.10991](#) [gr-qc].
- [45] V. Cardoso, J. L. Costa, K. Destounis, P. Hintz, and A. Jansen, Strong cosmic censorship in charged black-hole spacetimes: still subtle, *Phys. Rev. D* **98**, 104007 (2018), [arXiv:1808.03631](#) [gr-qc].
- [46] D. A. Easson, Quantum enforcement of strong cosmic censorship (2025), [arXiv:2511.05656](#) [gr-qc].